Articles in PresS. Am J Physiol Lung Cell Mol Physiol (April 20, 2017). doi:10.1152/ajplung.00063.2017

Klotho, an anti-aging molecule, attenuates oxidant-induced alveolar epithelial cell mtDNA damage and apoptosis

Seok-Jo Kim[1,2], Paul Cheresh[1,2], Mesut Eren[2], Renea P Jablonski[1,2], Anjana Yeldandi[3], Karen M Ridge[1,2], GR Scott Budinger[1,2], Dong-Hyun Kim[4], Myles S Wolf[5], Douglas Vaughan[2] and David W Kamp[1,2] †

[1]Department of Medicine, Division of Pulmonary & Critical Care Medicine, Jesse Brown VA Medical Center, Chicago, IL; [2]Department of Medicine, [3]Department of Pathology, and [4]Department of Radiology, Northwestern University Feinberg School of Medicine, Chicago, IL 60611. [5]Department of Medicine, Duke University School of Medicine, Durham, NC

*Address correspondence to David W. Kamp, M.D., Pulmonary and Critical Care Medicine, Northwestern University Feinberg School of Medicine, McGaw M-330, 240 E. Huron St., Chicago, IL, USA, 60611-3010, Phone: (312) 908-8163, Fax: (312) 908-4650,
E-mail: **d-kamp@northwestern.edu**

Running Title: Klotho attenuates AEC mitochondrial DNA damage

Keywords; mitochondrial DNA damage; oxidative stress, Klotho, alveolar epithelial cell, pulmonary fibrosis

Acknowledgement

This work is support by NIH-RO1 ES020357 (to D. W. K.) and Veterans Affairs Merit Award 2IO1BX000786-05A2 (to D. W. K.).

Abstract

Alveolar epithelial cell (AEC) apoptosis and inadequate repair resulting from 'exaggerated' lung aging and mitochondrial dysfunction are critical determinants promoting lung fibrosis. α-Klotho, which is an anti-aging molecule that is expressed predominantly in the kidney and secreted in the blood, can protect lung epithelial cells against hyperoxia-induced apoptosis. We reasoned that Klotho protects AEC exposed to oxidative stress in part by maintaining mitochondrial DNA (mtDNA) integrity and mitigating apoptosis. We find that Klotho levels are decreased in both serum and alveolar type II (AT2) cells from asbestos-exposed mice. We show that oxidative stress reduces AEC Klotho mRNA and protein expression whereas Klotho over-expression is protective while Klotho silencing augments AEC mtDNA damage. Compared to wild-type, Klotho heterozygous hypomorphic allele (*kl/+)* mice have increased asbestos-induced lung fibrosis due in part to increased AT2 cell mtDNA damage. Notably, we demonstrate that serum Klotho levels are reduced in WT but not mitochondrial catalase over-expressing (*MCAT*) mice 3 weeks following exposure to asbestos and that EUK-134, a MnSOD / catalase mimetic, mitigates oxidant-induced reductions in AEC Klotho expression. Using pharmacologic and genetic silencing studies, we show that Klotho attenuates oxidant-induced AEC mtDNA damage and apoptosis via mechanisms dependent upon AKT activation arising from upstream fibroblast growth factor receptor 1 (FGFR1) activation. Our findings suggest that Klotho preserves AEC mtDNA integrity in the setting of oxidative stress necessary for preventing apoptosis and asbestos-induced lung fibrosis. We reason that strategies aimed at augmenting AEC Klotho levels may be an innovative approach for mitigating age-related lung diseases.

Introduction

Klotho is an anti-aging gene originally discovered in 1997 when severe *Klotho* homozygous hypomorphic allele (*kl/kl*) mice demonstrated a rapidly progressive aging phenotype characterized by premature organ degeneration, emphysema, and early death (22, 29, 30). Notably, the *kl/kl* phenotype can be rescued by *Klotho* genetic manipulation or viral delivery and *Klotho* overexpression extends murine life span by 20-30% (13, 19, 30). Of the three Klotho protein family members (α, β, and γ), α-Klotho (named Klotho herein) is the most important and functions as a transmembrane protein that is predominantly produced in the kidney, choroid plexus, and to a lesser degree in other organs (28, 36). The extracellular domain of Klotho circulates as soluble Klotho exerting important pleiomorphic endocrine and paracrine functions including anti-fibrotic, anti-inflammatory, and anti-oxidant (i.e. inducing catalase and mitochondrial manganese superoxide dismutase [Mn-SOD]) effects in distant organs, including the lungs (1, 18, 30, 35, 39, 40, 59). Klotho acts as a co-receptor for fibroblast growth factor receptor (FGFR) and its ligand, fibroblast growth factor–23 (FGF23) to inhibit inorganic phosphate (Pi) reabsorption and vitamin D biosynthesis (21, 27, 58). There is evidence that diseases of oxidative stress (i.e. cancer, chronic kidney disease, the metabolic syndrome, etc.) are associated with low renal Klotho expression and circulating Klotho levels (1, 18, 30, 46, 59) but the pathophysiologic role of Klotho and relevance in pulmonary diseases is unknown.

Common lung diseases, such as chronic obstructive lung disease (COPD), idiopathic pulmonary fibrosis (IPF), asbestosis, combined pulmonary fibrosis and emphysema (CPFE), and others are age-related diseases associated with oxidative stress but the detailed molecular mechanisms involved are not established (6, 44, 51). Convincing evidence has emerged that impaired alveolar epithelial cell (AEC) injury and repair resulting from ‘exaggerated’ lung aging

and mitochondrial dysfunction are critical determinants of the lung fibrogenic potential of toxic agents, including asbestos fibers (5, 6, 32, 38, 44). Genome-wide association studies (GWAS) have shown a critical role for aberrant DNA repair pathways in patients with IPF (20, 44). Klotho prevents murine renal epithelial cell apoptosis and fibrosis by inhibiting TGFβ / Wnt signaling-induced DNA damage and protects murine lungs from acute hyperoxic lung injury by inhibiting A549 and primary human alveolar type I (ATI) epithelial cell DNA damage and apoptosis (39, 42). Furthermore, *kl/kl* mice have a lung phenotype (emphysema) and patients with COPD have reduced airway Klotho expression (12, 27) but it is unclear how Klotho is protective.

Accumulating evidence convincingly shows that mitochondrial DNA (mtDNA) damage occurs early following oxidative stress, such as from asbestos and tobacco smoke, contributing to their inflammatory, fibrogenic and malignant potential (4, 6, 24, 32). Further, mtDNA is more susceptible to oxidative damage than nuclear DNA due to the proximity of mtDNA to the ETC (4, 24, 26). We recently reported that mice deficient in an oxidative DNA repair enzyme, 8-oxoguanine DNA glycosylase (OGG1) have increased AT2 cell mtDNA damage, intrinsic apoptosis, and pulmonary fibrosis following asbestos exposure (7, 25) whereas mitochondrial catalase overexpressing transgenic (*MCAT*) mice, which have a prolonged life-span, are protected from asbestos- and bleomycin-induced AT2 cell mitochondrial reactive oxygen species (mtROS) production, mtDNA damage, apoptosis and lung fibrosis (23, 43). Aberrant FGF/FGFR signaling, which is implicated in the pathobiology of lung fibrosis, may act in part via effects on promoting DNA repair, including in AEC exposed to oxidative stress (3, 53, 56). Klotho attenuation of DNA damage may be one mechanism accounting for its protective effects against renal epithelial cell apoptosis and fibrosis (3, 17, 18, 42). However, the role of Klotho in

mitigating oxidant-induced AEC mtDNA damage important for promoting lung fibrosis is unknown.

We reasoned that Klotho protects AEC exposed to oxidative stress in part by maintaining mtDNA integrity and mitigating apoptosis. To address this hypothesis, we performed Klotho genetic and pharmacologic over- and under-expression *in vitro* studies and assessed asbestos-induced lung mtDNA damage and fibrosis in *Klotho* heterozygous hypomorphic allele (*kl/+*) mice that are partially deficient in Klotho yet, unlike *kl/kl* mice, are normal sized and with negligible alterations in circulating Pi or kidney function (11, 48). We report that oxidative stress (asbestos or H_2O_2) reduces AEC Klotho mRNA and protein expression and that Klotho over-expression attenuates oxidative stress-induced AEC mtDNA damage and apoptosis while Klotho silencing augments mtDNA damage and apoptosis. We find that mice exposed to asbestos for 3 weeks, as compared to a negative control particle (TiO_2), have reduced serum and AT2 cell Klotho levels. Interestingly, *kl/+* mice have increased asbestos-induced lung fibrosis as compared to their wild-type (WT) counterparts due in part to increased AT2 cell mtDNA damage and reduced lung and renal Klotho levels. A role for mitochondrial ROS in decreasing AEC Klotho expression was suggested by our findings that EUK-134, a MnSOD / catalase mimetic, mitigates oxidant-induced reductions in MLE-12 Klotho expression and that *MCAT* mice, as compared to WT, have higher serum Klotho levels 3 weeks following asbestos exposure. We also provide support for a mechanistic role for Klotho-induced AKT signaling acting down-stream of Fibroblast growth factor receptor 1 (FGFR1), not Insulin-like growth factor receptor (IGFR), signaling in preventing oxidant-induced AEC mtDNA damage and apoptosis. Taken together, these studies implicate an important role for the Klotho/FGFR1/AKT axis in maintaining AEC cell mtDNA integrity in the setting of oxidative stress that is crucial for preventing AEC

apoptosis and pulmonary fibrosis. Further, these studies suggest Klotho as a potentially novel strategy in protecting AECs from oxidative stress as seen in asbestosis as well as other age-related lung diseases (i.e. emphysema, asbestosis, CPFE, IPF, etc).

Materials and Methods

***Reagents*:** Crocidolite and amosite amphibole asbestos fibers employed were Union for International Cancer Control (UICC) reference standards kindly supplied by Dr. Andy Ghio (U.S. Environmental Protection Agency) as characterized previously (37). EUK-134 was purchased from Cayman Chemical (Ann Arbor, MI). Recombinant Klotho was purchased from R&D Systems (Minneapolis, MN). All other reagents were purchased from Sigma-Aldrich (St. Louis, MO) unless specified. Anti-Klotho and GAPDH antibody were purchased from Santa Cruz (Biotechnology, Inc., Dallas, TX). Anti-cleaved caspase-9, phospho-AKT and total AKT antibodies were purchased from Cell Signaling Technology (Danvers, MA).

Cell Culture: Murine AT2 cells were isolated as we previously described (7, 23, 25). The AT2 cells obtained routinely display > 90% purity as assessed by pro-SFTPC (Millipore, Temecula, CA) immunofluorescence analysis and > 95% viability via trypan blue staining. The A549, MLE-12 and RLE-6TN cell lines were purchased from the American Type Culture Collection (ATCC, Manassas, VA, USA). All cultured AECs were maintained in DMEM (Invitrogen, Grand Island, NY) with 2mM *L*-glutamine supplemented with 10% fetal bovine serum, penicillin (100 units/mL) and streptomycin (100 μg/mL). Cells were plated in 6-well plates or 100-mm dishes and grown to confluence before adding asbestos or H_2O_2 for up to 24 h as previously described (23, 25) and harvesting protein extracts for Western blotting or, in separate experiments, obtaining nuclear and mitochondrial DNA for DNA fragmentation and a

PCR-based DNA damage assay.

Western Blot: Cell lysates were collected and immunoblotted as described (25) using antibodies directed against CC-9 (Cell Signaling Technology, Danvers, MA), Klotho (Abcam, Cambridge, MA), and GAPDH (Santa Cruz). The protein bands were enhanced and visualized by luminol-based detection using ECL Western Blotting Detection Reagent (GE Healthcare Bio-Sciences, Pittsburgh, PA) and quantified by Image J software.

Gene expression analysis: Total RNA was extracted from MLE-12 cells using TRIzol (Thermo Fisher Scientific, Waltham, MA) according to the manufacturer's instructions. Real-time quantitative PCR for murine Klotho (Mm.PT.58.29356714) and murine β-actin (Mm.PT.39a.22214843.g) was performed using the TaqMan Expression PrimeTime Std® qPCR Assay from Integrated DNA Technologies, Inc. (Coralville, IA) and performed using the ABI7300 Real time PCR system (Applied Biosystems, Foster City, CA). All experiments were performed according to the manufacturer's protocol.

Plasmid construction for Klotho-WT expression: Complementary DNAs encoding the full length human Klotho was obtained from Addgene (Cambridge, MA). The pcDNA3.1/V5/His-TOPO empty vector control was purchased from Thermo Fisher Scientific (Waltham, MA). To generate cells that transiently express the full length Klotho proteins, the plasmids were transfected into MLE-12 cells using Lipofectamine 2000 (Thermo Fisher Scientific) according to the manufacturer's recommendations. The transfection efficiency is > 95%. 48 hours post-transfection, cells were subject to Western blot using anti-His antibody (Abcam, Cambridge, MA) to detect overexpressed Klotho tagged with His and DNA fragmentation as well as mtDNA damage.

Gene silencing: Klotho, AKT, IGFR, FGFR1-specific siRNA and scrambled (control)

siRNA were purchased from Integrated DNA Technologies and then transiently transfected into MLE-12 cells using Lipofectamine RNAiMax (Invitrogen) according to the manufacturer's recommendations. After transfection for 48 h, the cells were tested for Western blot and DNA fragmentation as well as mtDNA damage.

Determination of soluble Klotho: Blood samples from mice were taken under anesthesia with 3% isoflurane (Butler Animal Health, Dublin, OH), and the culture media from MLE-12 cells were collected by centrifugation. The concentration of soluble Klotho in serum, murine lungs, and cell culture media was determined by Klotho ELISA kit (MyBioSource, Inc., San Diego, CA) according to the manufacturer's specifications.

Quantitative PCR-based mtDNA damage assay: Nuclear and mtDNA damage were assessed by Q-PCR as previously described (23, 25). Briefly, genomic DNA was extracted using the Qiagen Genomic-Tip 20/G and Qiagen DNA Buffer Set (Qiagen, Gaithersberg, MD) per the manufacturer's protocol. PCR was performed using Ex-Taq (Clontech, Mountain View, CA) with specific primers to amplify a mitochondrial genomic fragment in both short and long form and nuclear DNA (β-globin) as previously described (23, 25). DNA was quantified by Pico-Green (Thermo Fisher Scientific) using the FL600 microplate fluorescence reader with excitation and emission wavelengths of 485 nm and 530 nm, respectively. The data obtained from the mitochondria small fragment were used to normalize the results of the mitochondria long fragment. The number of mitochondrial lesions was calculated by the equation, $D = (1 - 2^{-(\Delta long-\Delta short)}) \times 10{,}000$ (bp)/size of the long fragment (bp).

DNA fragmentation assay: Apoptosis was evaluated using a histone-associated DNA fragmentation (mono- and oligonucleosomes) Cell Death Detection ELISA^{PLUS} kit (Sigma-Aldrich) as previously described using the manufacturer's protocol (7, 25).

Asbestos-induced murine lung fibrosis: All the animal studies were approved by the Institutional Animal Use and Care Committees (IACUC) at Northwestern University and the Jesse Brown VA Medical Center. Male and female 8- to 10- week old C3H/C57Bl/6J wild-type (WT), *kl/+*, and *MCAT* (C57Bl/6J background; kindly provided by Peter S. Rabinovitch and C. Michael Hart (43)) mice were used for lung fibrosis studies as we have previously described (7, 23). Stock solutions (2 mg/mL) of crocidolite asbestos was prepared in phosphate buffered saline (PBS) and 15 mM HEPES (Sigma-Aldrich) and sonicated at 40% power (Sonicator: Branson, Danbury, CT) for 8 minutes to disrupt fiber clumps. Eight to ten week-old male or female WT or *kl/+* mice were anesthetized with 3% isoflurane, intubated orally with a 20-gauge angiocath (BD, Sandy, UT), and 100 μg of crocidolite asbestos or TiO_2 (negative control particle) suspended in 50 μL sterile PBS was instilled in 2 equal aliquots given 2 minutes apart. After each aliquot the mice were placed in the right and then the left decubitus position for 10-15 seconds.

Lung collagen detection: For soluble collagen measurement, the left lung was homogenized with acetic acid using a polytron (Kinematica, Bohemia, NY) then a dounce homogenizer and cleared by centrifugation. Equal volumes of cleared homogenate were subject to the Sircol assay for soluble collagen based on a modified Picosirius Red collagen precipitation assay as previously described by our group (7, 23).

Fibrosis scoring system: The lung fibrosis score, which is based upon the severity and extent of lung fibrosis and not inflammation present in the peribronchial and interstitial tissues, was assessed by one of us who is a pulmonary pathologist (AY) as previously described (7, 23). Lungs were assigned a severity score from 0 (no fibrosis) to 4 (severe fibrosis) while the extent of involvement was quantified on a scale of 1 (occasional alveolar duct and bronchiole

involvement) to 3 (more than half of the alveolar ducts and respiratory bronchioles involved). The fibrosis score was calculated as the severity (0-4) multiplied by the extent (1-3).

Statistical analysis: All results are determined as the means ± S.E.M. for three or more independent experiments. A two-tailed Student's t-test was used to assess the significance of differences between two groups. Statistical differences among groups were determined using one-way ANOVA and Tukey's multiple comparison test using Graph-Pad Prism Software (Graph Pad Prism Inc. La Jolla, CA). Probability values < 0.05 were considered significant.

Results

Oxidative stress depletes AEC cell Klotho protein & mRNA expression. To determine if oxidative stress alters Klotho expression, AECs (A549, MLE-12 and RLE-6TN cells) were exposed to amosite asbestos (5-25 μg/cm^2) or H_2O_2 (100-200 μM) for 24h and assessed for protein and mRNA expression (**Fig 1**). We noted that oxidative stress (asbestos and H_2O_2) reduced Klotho protein expression (**Fig 1A**) and secretion into the media (**Fig 1B**). Furthermore, AEC Klotho mRNA levels were decreased by oxidative stress in a time-dependent manner (**Fig 1C**). These results show that oxidative stress decreases AEC Klotho protein expression, secretion and mRNA expression.

Klotho attenuates oxidative stress-induced mtDNA damage and apoptosis in AECs. To assess whether Klotho attenuates AEC mtDNA damage and apoptosis, MLE-12 cells were transiently transfected with empty vector (EV) control or Klotho-WT plasmids for 48h and then oxidant (amosite asbestos or H_2O_2)-induced mtDNA damage and apoptosis (measured by the level of cleaved caspase-9 (CC-9) and DNA fragmentation) were assessed at 24h. Compared to EV controls, Klotho-WT augmented Klotho protein expression resulting in decreased oxidant-

induced mtDNA damage and intrinsic apoptosis (**Fig 2A-2C**). To assess whether recombinant Klotho (reKlotho) attenuates AEC mtDNA damage and apoptosis, MLE-12 cells were pretreated with reKlotho for 6h and then oxidant (amosite asbestos or H_2O_2)-induced mtDNA damage and apoptosis (DNA fragmentation and CC-9 expression) were assessed at 24h. Compared to controls, reKlotho significantly reduced oxidant-induced mtDNA damage and apoptosis (**Fig 2D-2F**). Similar findings were also noted in A549 cells (data not shown).

To assess whether Klotho deficiency augments AEC mtDNA damage, MLE-12 cells were exposed to scramble or Klotho siRNA for 48h and then oxidant (amosite asbestos or H_2O_2)-induced mtDNA damage and apoptosis were assessed at 24h. Compared to controls, Klotho siRNA blocked Klotho protein expression, which increased mtDNA damage and apoptosis in control MLE-12 cells (**Fig 3;** 0 v. 0.4 lesions per 10 kb, respectively, $p< 0.05$). Moreover, Klotho silencing augmented AEC mtDNA damage and apoptosis in the presence of asbestos or H_2O_2, although these differences in mtDNA damage (0.44±0.13, 0.65±0.10 and 0.68±0.12 lesions per 10kb frequency per fragment, respectively) did not reach statistical significance. Taken together, both genetic and pharmacologic Klotho overexpression attenuate oxidative stress-induced AEC mtDNA damage and intrinsic apoptosis while the loss of Klotho enhances oxidative stress-induced AEC mtDNA damage and apoptosis.

Klotho levels are decreased in the serum and AT2 cells from asbestos-exposed mice. Circulating Klotho acts in part via an endocrine effect (1, 18, 30, 46, 59). To test whether circulating Klotho is reduced during lung fibrosis, we measured the level of soluble Klotho in mice using the asbestos model of lung fibrosis as we previously described (7, 23). As compared to TiO_2, crocidolite asbestos-exposed WT mice had reduced serum Klotho levels at 3 weeks, a time point where there is significant lung fibrosis and AT2 cell mtDNA damage and apoptosis

(**Fig 4A**). Notably, AT2 cells from asbestos-exposed mice also had decreased Klotho levels by ~40% as compared to TiO_2, the negative control particle (**Fig 4B**). As an alternative *in vitro* approach, we isolated primary AT2 cells from untreated mice and exposed them to oxidative stress using amosite asbestos (25 μg/cm^2) or H_2O_2 (200 μM) for 24h. Consistent with our *in vivo* data, both asbestos and H_2O_2 reduced Klotho expression levels (**Fig 4C**)**.** Taken together, these data show that oxidative stress decreases circulating Klotho levels in the serum as well as AT2 cells.

Asbestos-induced pulmonary fibrosis is augmented in kl/+mice as compared with WT mice. Due to the small size of the homozygous *kl/kl* mice, we studied asbestos-induced pulmonary fibrosis using *kl/+* mice which are of normal size yet with >50% reduction in Klotho expression compared to WT but with insignificant alterations of serum Pi or kidney function (11, 48). To assess whether Klotho deficiency augments asbestos-induced pulmonary fibrosis, we compared WT and *kl/+*mice 3 weeks following a single IT instillation of TiO_2 (100 μg/50 μl) or crocidolite amphibole asbestos (100 μg/50 μl). Compared to TiO_2, crocidolite significantly augmented pulmonary fibrosis in WT mice as expected as assessed by histology, fibrosis scoring, and the Sircol assay for lung collagen (**Fig 5A-C**). Notably, asbestos-induced lung fibrosis was further significantly increased in *kl/+*mice as assessed by histopathology, lung fibrosis scoring and lung collagen levels (**Fig 5A-C**). Additionally, to directly test whether *kl/+*increases asbestos-induced AT2 cell mtDNA damage, we exposed WT and *kl/+* mice to IT-instilled TiO_2 or crocidolite asbestos for 3 weeks and then evaluated mtDNA damage in primary isolated AT2 cells. As expected, AT2 cells from WT mice had increased mtDNA damage following exposure to crocidolite asbestos as compared to TiO_2 (**Fig 5D**). Interestingly, AT2 cells isolated from *kl/+* mice exposed to our inert control (TiO_2) had increased mtDNA damage, which was amplified

following asbestos treatment (**Fig 5D**). Together, these findings show that asbestos-induced lung fibrosis and mtDNA damage is significantly augmented in asbestos-exposed *kl/+* mice as compared to their WT counterparts.

Mitochondrial catalase and EUK-134 diminish the depletion of Klotho exposed to oxidative stress. We recently reported that asbestos-induced lung fibrosis is attenuated in *MCAT* mice in association with reduced AT2 cell mtROS production, mtDNA damage and apoptosis (23). To determine whether the reductions in soluble Klotho levels that occur in the setting of asbestos-induced lung fibrosis are dependent on mtROS, we measured the circulating Klotho level in serum from WT and *MCAT* mice 3 weeks following a single IT instillation of TiO_2 or crocidolite asbestos. In accord with our findings in Fig 4A, serum Klotho levels were decreased in crocidolite-exposed WT mice as compared to TiO_2 (**Fig 6A**). Notably, serum Klotho levels from asbestos-exposed *MCAT* mice was negligibly reduced as compared to TiO_2-treated WT mice (**Fig 6A**), suggesting a critical role for mtROS in reducing circulating Klotho. To further address the role of mtROS, we explored whether EUK-134, an MnSOD / catalase mimetic known to reduce asbestos-induced mtROS and mtDNA damage (23, 45) attenuates oxidative stress-induced reductions in Klotho expression. MLE-12 cells were pretreated with EUK-134 (20 μM) for 6h and then Klotho expression following amosite asbestos- or H_2O_2-induced oxidative stress was assessed at 24h. Compared to controls, EUK-134 mitigated oxidant-induced decreases in MLE-12 cell Klotho protein expression following exposure to either asbestos or H_2O_2 (**Fig 6B**) and soluble Klotho as measured via ELISA (**Fig 6C**). Collectively, these findings along with our previous studies suggest that mtROS are crucial for promoting the reduction in asbestos-induced AEC Klotho expression that can promote AEC mtDNA damage and apoptosis that are important for augmenting lung fibrosis.

AKT is important in the protective effects of Klotho against oxidative stress-induced AEC mtDNA damage. Given that the neuroprotective effects of Klotho are mediated via AKT (60) and that asbestos-induced AEC apoptosis is associated with reduced AKT activation (2), we reasoned that the AEC protective effects of Klotho are dependent upon AKT activation. To determine whether AKT or another signaling pathway primarily mediates Klotho's AEC mtDNA protective effects in the setting of oxidative stress, MLE-12 cells were pre-incubated with an AKT inhibitor (GSK690693, 10 μM), ERK inhibitor (U0125, 10 μM), JNK inhibitor (SP600125, 5 μM) or p38 MAPK inhibitor (SB203580, 5 μM) for 6h and exposed to amosite asbestos (25 $\mu g/cm^2$) or H_2O_2 (200 μM) for 24h. Compared to DMSO controls (0.01%), an AKT inhibitor augmented asbestos-induced mtDNA damage **(Fig 7A)** while the other inhibitors had negligible effects **(Fig 7A).** Consistent with others working with A549 cells (2), we found that asbestos reduced MLE-12 cell AKT activation as assessed by phosphorylated AKT expression **(Fig 7B)**. To further explore the effects of inhibiting AKT signaling on AEC mtDNA damage in the setting of oxidative stress, MLE-12 cells were transfected with scramble or AKT-targeted siRNA for 48h before being exposed to asbestos (25 $\mu g/cm^2$) or H_2O_2 (200 μM) for 24h in the absence or presence of reKlotho and then mtDNA damage was assessed. Similar to an AKT pharmacologic inhibitor, silencing of AKT augmented mtDNA lesions under untreated conditions as compared to scamble controls and mtDNA damage was further augmented after exposure to asbestos or H_2O_2 **(Fig 7C)**. Notably, AKT silencing completely blocked the protective effects of re-Klotho against oxidant-induced MLE-12 cell mtDNA damage (**Fig 7D**). Taken together, our findings firmly support that the mechanism by which Klotho prevents oxidant-induced AEC mtDNA damage requires AKT activation.

FGFR, but not IGFR, is necessary for the protective effects of Klotho to oxidative stres-

induced mtDNA damage in AECs. Although unclear in the lungs, there is evidence that Klotho activates AKT via upstream FGFR1 or IGFR signaling in neuronal and cardiac cells (3, 8, 15, 50, 55, 60). To determine which receptor-mediated signaling pathway mediates the protective effect of Klotho in AEC, we transfected MLE-12 cells with Scramble control, FGFR1- or IGFR-specific siRNA for 48h before being exposed to asbestos (25 μg/cm^2) or H_2O_2 (200 μM) for 24h in the absence or presence of reKlotho and then mtDNA damage was assessed. Compared to scramble controls, cells treated with FGFR1 or IGFR siRNA had increased mtDNA damage under basal conditions and these effects were further enhanced after exposure to asbestos or H_2O_2 (**Fig. 7E**). Importantly, FGFR1 silencing completely blocked the protective effects of reKlotho against oxidant-induced AEC mtDNA damage while IGFR-silencing had negligible effects (**Fig. 7E**). Collectively, these data firmly support that the protective effects of Klotho against oxidant-indcued AEC mtDNA damage are mediated via FGFR1 and not IGFR signaling.

Discussion

Accumulating evidence suggests that AEC injury, in part from mtDNA damage, is a key target that integrates both pro-aging and cell survival / death signaling following exposure to fibrogenic agents, such as asbestos (see for Reviews: (6, 24, 44, 51). In this study, we identify a crucial role for the Klotho-FGFR-AKT axis in preventing oxidative stress-induced AEC mtDNA damage. We demonstrate that oxidative stress (asbestos or H_2O_2), a key mediator underlying the aging process in IPF, asbestosis, and other age-related lung diseases (6, 24, 44, 51), decreases Klotho levels in AEC as well as in the serum of asbestos-exposed mice. We show that Klotho over-expression, using genetic or pharmacologic approaches, attenuates oxidant-induced AEC mtDNA damage and intrinsic apoptosis while AEC Klotho depletion using siRNA *in vitro* or *in*

vivo using *Kl/+* mice enhances oxidant-induced mtDNA damage and asbestos-induced lung fibrosis. A role for mtROS mediating the reductions in Klotho is suggested by our findings that serum Klotho levels are preserved in asbestos-exposed *MCAT* as compared to WT mice and that EUK-134 preserves AEC Klotho expression *in vitro*. Finally, we provide evidence that the mechanism by which Klotho mitigates oxidant-induced AEC mtDNA damage is mediated by AKT signaling via the FGFR pathway.

A major finding in this study is that oxidative stress from either amphibole (amosite or crocidolite) asbestos fibers (exogenous source) or H_2O_2 (endogenous source) reduces AEC Klotho protein and mRNA expression *in vitro* in a variety of AEC types (A549, MLE-12 and RLE-6TN; **Fig 1**) as well as *in vivo* in the serum of asbestos-exposed WT mice and supernatant of primary isolated AT2 cells (**Fig 4**). Klotho, which is an anti-aging protein primarily made in the kidney and to a lesser degree in other organs, exerts important hormonal functions including anti-fibrotic, anti-inflammatory and anti-oxidant effects in distant organs, including the lungs (1, 18, 21, 28, 30, 35, 39, 40, 59). Our data showing that asbestos exposure reduces serum Klotho levels adds to the growing evidence that serum Klotho levels are reduced in diseases of oxidative stress such as cancer and chronic kidney disease (16, 46).

Several lines of evidence in this study firmly implicate that Klotho has a key role in maintaining AEC mtDNA integrity in the setting of oxidative stress. First, Klotho over-expression studies using transient transfection of a plasmid expressing Klotho as well as re-Klotho both decreased oxidative stress (amosite asbestos and H_2O_2)-induced AEC mtDNA damage and apoptosis as assessed by DNA fragmentation and CC-9 activation (**Fig 2**). Second, Klotho silencing studies using Klotho siRNA augmented AEC mtDNA damage at baseline as compared to scramble controls and oxidative stress from asbestos or H_2O_2 further enhanced these

deleterious effects (**Fig 3**). Finally, to address the *in vivo* relevance of our *in vitro* findings that Klotho deficiency promotes AEC mtDNA damage, we used the asbestos-induced model of lung fibrosis that we have previously shown is associated with increased AEC mtDNA damage and apoptosis (7, 23). Because *kl/kl* mice that are completely devoid of Klotho were not feasible to study as they die at a young age and are too small for asbestos IT-instillations, we utilized the *kl/+* heterozygotes that have a 50% reduction in Klotho serum levels yet have a normal size, renal function, and negligible alterations of serum Pi levels (11, 48). Interestingly, we found that the *kl/+* mice, as compared to WT, are more susceptible to asbestos-induced pulmonary fibrosis as assessed by histology and lung fibrosis score and collagen production (**Fig. 5A-C**). Notably, as compared to WT, primary isolated AT2 cells from *kl/+* mice have increased mtDNA damage at baseline 3 weeks following exposure to an inert particle TiO_2 and this is further augmented by crocidolite asbestos, which we have shown reproducibly causes lung fibrosis (**Fig 5D**) (7, 23). Our data showing that lung fibrosis in *kl/+* mice exposed to asbestos are only modestly worse than WT mice suggests that the 50% reduction in serum Klotho levels may be sufficient to augment fibrotic signaling. Although the mechanism accounting for this finding is not fully established, our data suggests that this is due in part by the increased AEC mtDNA damage noted in *kl/+* mice, which concurs with our findings implicating AEC mtDNA integrity in other transgenic mouse lung fibrosis models including *Ogg1*-deficient and *MCAT* mice (7, 23). Our data are in accord with studies showing that Klotho prevents oxidant (H_2O_2, hyperoxia)-induced murine renal epithelial, A549, and primary human AT1 cell DNA damage and apoptosis (39, 42, 47) and extend these studies by implicating mtDNA as a key Klotho target. Taken together, these findings support a novel role for Klotho in maintaining AEC mtDNA integrity. Although the importance of Klotho for maintaining normal lungs under control conditions is established by the

finding of emphysema in *kl/kl* mice maintained in a sterile environment (10, 22, 29), further studies will be of interest ascertaining the molecular mechanisms by which Klotho modulates AEC mtDNA damage following exposure to environmental insults (i.e. asbestos, tobacco, etc) that promote emphysema with and without lung fibrosis (i.e. COPD, IPF, CPFE, asbestosis).

The mechanism underlying the protective effects of Klotho against oxidative stress-induced AEC mtDNA damage is not entirely established but we explored several possibilities. First, a role for mtROS is suggested by two lines of evidence: (1) compared to WT mice, circulating Klotho levels are preserved in asbestos-exposed *MCAT* mice, which we previously showed are protected from asbestos-induced AEC mtROS production, mtDNA damage, apoptosis, and lung fibrosis (**Fig 6A**; (23) and (2) EUK-134, a MnSOD/catalase mimetic that we have reported reduces mtROS production (45), mitigates oxidant-induced reductions in Klotho expression (**Fig 6B and C**). We reason that our data implicating mtROS in reducing serum Klotho expression in the setting of environmental stress (i.e. asbestos) may in part account for the extended life-span of *MCAT* mice (43). Further studies determining the precise mechanism by which mtROS reduce Klotho expression will be of interest given that mtDNA damage arising from mtROS or altered mtDNA repair processes have been prominently implicated in the aging process (9, 24, 49, 52). Klotho upregulates endogenous antioxidant defenses, including SOD2, which are vital in mitigating apoptosis, cellular senescence and oxidative injury suggesting an important feedback loop between Klotho and oxidative stress (47, 58).

Second, our studies identify activated AKT as the critical kinase signaling pathway mediating the protective effects of Klotho against AEC mtDNA damage. This conclusion is supported by our observations that AKT inhibition using either a pharmacologic agent or silencing of AKT using siRNA each augmented oxidant-induced AEC mtDNA damage (**Fig. 7A**

and 7C). In contrast, pharmacologic inhibition of ERK, JNK, or p38 had negligible effects of AEC mtDNA damage at baseline as well as following oxidative stress (**Fig 7A**). Interestingly, AKT silencing completely blocked the protective effects of reKlotho against oxidative stress-induced AEC mtDNA damage, indicating that AKT is essential for mediating the beneficial effects of Klotho on mtDNA integrity. It is possible that Klotho's AKT-dependent beneficial effects noted herein are unique to epithelial cells since AKT signaling has the paradoxical effect of promoting cell survival or death depending upon the cell type. For example, pathogenic activation of AKT is evident in fibroblasts and macrophages isolated in a murine model of bleomycin-induced lung fibrosis or in fibroblasts of IPF patients (31, 33, 57). In contrast, PI3K/AKT signaling is required to attenuate oxidant-induced cell injury in lung epithelial, retinal pigment epithelial, and neuronal cell injury, including asbestos-induced AEC apoptosis (2, 34, 41, 54). AKT deficiency promotes oxidative DNA damage by decreasing DNA repair in renal cells (14). Those data are in accord with our finding that silencing of AKT augments MLE-12 cell mtDNA damage and that asbestos augments these effects **(Fig. 7C)**.

Third, we showed that FGFR1, not IGFR, upstream signaling is responsible for mediating Klotho-dependent AKT activation that limits oxidative stress-induced AEC mtDNA damage. This is supported by our data showing that the protective effect of reKlotho in mitigating oxidative stress-induced mtDNA damage was abolished following silencing of FGFR1 but not by silencing IGFR (**Fig. 7E**). Our findings are in accord with studies showing that FGFR1-dependent mechanisms mediate Klotho's protective effects against renal epithelial cell apoptosis and fibrosis in part by inhibiting DNA damage and activating TGFβ / Wnt signaling (3, 18, 40, 42) as well as our previous studies showing that FGF7 (KGF) and FGF10 reduce AEC injury by augmenting DNA repair (53, 56). Further, our findings concur with studies showing that AKT

signaling via FGFR1 is crucial for mediating the neuroprotective effect of Klotho (60). Although IGFR-AKT signaling appears important for aging-associated diseases, including heart failure (15, 50) and breast cancer (55), our data do not support a role for IGFR-AKT signaling in mediating the protective effects of Klotho against oxitaive stress-induced AEC mtDNA damage. Collectively, this suggests that the protective effect of Klotho is mediated via the FGFR1-AKT pathway.

In summary, we demonstrate a novel role for the Klotho-FGFR1-AKT axis in attenuating oxidant-induced AEC mtDNA damage and that, compared to WT, *kl/+* mice are more prone to asbestos-induced AEC mtDNA damage as well as lung fibrosis. A crucial role for Klotho in preserving AEC mtDNA integrity is supported by our findings that include: (i) oxidative stress (asbestos or H_2O_2) reduces AEC Klotho levels *in vitro* as well as *in vivo* in the serum of asbestos-exposed mice; (ii) Klotho over- and under-expression studies showing a direct relationship between Klotho levels and AEC mtDNA integrity; and (iii) FGFR1 and AKT silencing block the protective effects of Klotho against oxidative stress-induced AEC mtDNA damage. We present evidence for a role of mtROS in mediating the reductions in Klotho but further studies will be necessary to define the precise molecular pathways involved. A hypothetical model depicting the major findings noted in this study is shown in **Figure 7F**. Oxidative stress following asbestos exposure and other environmental toxins can decrease Klotho expression that renders AEC susceptible to oxidant-induced mtDNA damage and intrinsic apoptosis important in the pathogenesis of lung fibrosis. Further studies will be important for characterizing the detailed molecular mechanisms involved as well as the relevance in human diseases and other markers for IPF (e.g., TGFβ1, ECM, or MMPs). We reason that Klotho deficiency resulting in aberrant FGFR1/AKT signaling in the pathobiology of lung fibrosis represents a novel therapeutic target

462 for preventing common lung diseases of aging including COPD, IPF, asbestosis, CPFE, and
463 others.

Figure legends

Fig.1. Oxidative stress depletes Klotho expression in several types of AECs.

(A) AEC Klotho protein expression following amosite asbestos (5-25 μg/cm^2) or H_2O_2 (100-200 μM) exposure for 24h. GAPDH is a loading control. A densitometric analysis using GAPDH as a loading control from 3 experiments is shown. (B) Secreted AEC Klotho level following asbestos or H_2O_2 exposure for 24h. (C) A549 and MLE-12 cell mRNA expression for Klotho following asbestos exposure as assessed by Q-PCR. The values are represented as mean ± SEM. (*P<0.05 v. Control; n=3).

Fig. 2. Klotho overexpression and recombinant Klotho prevent MLE-12 cell mtDNA damage and intrinsic apoptosis exposure to asbestos or H_2O_2.

Klotho overexpression (A-C) and recombinant Klotho (D-F) blocks oxidative stress-induced cleaved caspase-9, mtDNA damage and intrinsic apoptosis caused by amosite asbestos (25 μg/cm^2) or H_2O_2 (200 μM) for 24 h in MLE-12 cells. A, Klotho overexpression is measured by anti-His antibody. Cleaved-caspase-9 in total cell lysate was assessed by Western blotting showing representative figure. A densitometric analysis using GAPDH as a loading control from 3 experiments is shown. B, mtDNA damage was performed by Q-PCR based measurement using isolated whole genomic DNA from each condition. C, Intrinsic apoptosis was detected by ELISA assay using Cell death detection kit. The values are represented as mean ± SEM. (*P<0.05 v. Control, +P<0.05 v. empty vector or PBS vehicle ASB/ H_2O_2; n=3).

Fig.3. Klotho Deficiency Augments Asbestos-Induced AEC mtDNA Damage and intrinsic apoptosis.

Control siRNA or Klotho siRNA was transfected to MLE-12 cells for 48 h , and were exposed to amosite asbestos (25 μg/cm^2) or H_2O_2 (200 μM) for 24 hours. Cleaved-caspase-9 in total cell lysate as well as Klotho expression were assessed by Western blotting showing representative figures and a densitometric analysis using GAPDH as a loading control (A), and mtDNA damage was performed by Q-PCR based measurement using isolated whole genomic DNA from each condition (B). Intrinsic apoptosis was detected by ELISA assay using Cell death detection kit (C). The values are represented as mean ± SEM. (*P<0.05 v. Control, +P<0.05 v. Scramble; n=3).

Fig 4. Asbestos Reduces Serum and AT2 Cell Klotho Levels as Compared to TiO_2 in WT Mice.

Serum (A) and primary AT2 cells (B) were isolated from WT mice at three weeks after intratracheal instillation with TiO_2 or crocidolite asbestos. (C) Primary AT2 cells were isolated from WT mice, then exposed to amosite asbestos or H_2O_2. ELISA was performed to detect Klotho level at each condition. n = 3 mice per group. Data are presented as means ± SEM (*$p<0.05$ vs. TiO_2 or Control).

Fig 5. *kl/+* mice exposed to asbestos presents the increase of lung fibrosis and AT2 cell mtDNA damage compared to WT.

After intratracheal instillation with TiO_2 or crocidolite asbestos for three weeks, serial lung sections from age-mached WT and *kl/+* mice were subject to Masson's trichrome stain (A), lung fibrosis scores (B) and lung collagen levels (C). (A) Representative histology is shown from 4 to 9 mice in WT and *kl/+* mice after treatment. (B) The fibrosis score = (severity: 0–4)×(extent: 1–3). *$p<0.05$ vs. TiO_2, +$p<0.05$ vs. WT+crocidolite asbestos, n =3-4. (C) Lung collagen levels as assessed by Sircol assay. *$p<0.05$ vs. TiO_2, +$p<0.05$ vs. WT+crocidolite asbestos. n= 3-9. D, and mtDNA damage were assessed by a fluorescent-based PCR mtDNA damage assay using genomic DNA of primary AT2 cells isolated from the lungs of WT and *kl/+* mice three weeks after IT instillation of TiO_2 or crocidolite asbestos. Graph express as the ratio of lesion frequency per fragment as compared to WT AT2 cells exposed to control – TiO_2). *$p < 0.05$ vs. TiO_2, +$P < 0.05$ vs. WT + crocidolite asbestos, #$p<0.05$ vs. *kl/+* mice+crocidolite asbestos, n = 3.

Fig 6. Mitochondrial catalase and its mimetic, EUK-134, protects oxidanat-induced Klotho reduction in serum from WT and MCAT mice as well as MLE-12 cells.

(A) Serum were collected from WT and *MCAT* mice at three weeks after intratracheal instillation with TiO_2 or crocidolite asbestos, and Klotho level was measured by ELISA. B and C, conlfuent MLE-12 cells were incubated with EUK-134 (20 μM) for 3 hours, and then were exposed to amosite asbestos (25 $\mu g/cm^2$) or H_2O_2 (200 μM) for 24 hours. Cell lysate from each group were shown to Klotho level performed with Western blotting showing representative image with the densitometric analysis of Klotho/GAPDH relative to untreated control (B) and ELISA (C). n = 3 mice or MLE-12 cells per group. Data are presented as means ± SEM (*$p<0.05$ vs. WT+TiO_2 or

PBS+Control).

Fig 7. The Klotho/FGFR/AKT axis regulates oxidative stress-induced AEC mtDNA damage and apoptosis.

(A), Effect of signaling pathway inhibitors on oxidant-induced AEC mtDNA damage. MLE-12 cells were pre-incubated with an AKT inhibitor (GSK690693, 10 μM), ERK inhibitor (U0125, 10 μM), JNK inhibitor (SP600125, 5 μM) or p38 MAPK inhibitor (SB203580, 5 μM) for 6h, and exposed to amosite asbestos (25 $\mu g/cm^2$) or H_2O_2 (200 μM) for 24h. mtDNA damage was performed by Q-PCR based measurement. (*$p<0.05$ vs. DMSO) (B) Phospho-AKT is inhibited in asbestos-exposed MLE-12 cells. MLE-12 cells were exposed to amosite asbestos (5 or 25 $\mu g/cm^2$) for 1h or 3h. Cell extracts were isolated and phospho-AKT level was evaulated by Western Blotting showing representative image and semi-quantitative analyzed graph. (*$P<0.05$ v. Control, n=3) (C and D) AKT1 silencing increses mtDNA damage and blocks the protective effects of recombinant Klotho in oxidant-induced MLE-12 cells. Cells were trasfected with siRNA targeted to AKT1, and then recombinant Klotho was preincubated for 3h and exposed to amosite asbestos (25 $\mu g/cm^2$) or H_2O_2 (200 μM) for 24h. mtDNA damage was performed by Q-PCR based measurement using isolated whole genomic DNA from each condition. The values are represented as mean ± SEM. (*$P<0.05$ v. Scr/Control, +$P<0.05$ siAKT v. siAKT+reKlotho; n=3) (E) FGFR1, but not IGFR, silencing blocks reKlotho's protective wffects against oxidant-induced AEC mtDNA damage. MLE-12 cells were trasfected with siRNA targeted to IGFR or FGFR1, and then recombinant Klotho was preincubated for 3h and exposed to amosite asbestos (25 $\mu g/cm^2$) or H_2O_2 (200 μM) for 24h. mtDNA damage was performed by Q-PCR based measurement using isolated whole genomic DNA from each condition. The values are represented as mean ± SEM. (*$P<0.05$ v. Scr/Control, +$P<0.05$ siIGFR v. siIGFR+reKlotho; n=3). (F) Hypothetical model by which Klotho prevents oxidant-induced AEC mtDNA damage, apoptosis, and lung fibrosis.

References

1. **Asai O, Nakatani K, Tanaka T, Sakan H, Imura A, Yoshimoto S, Samejima K, Yamaguchi Y, Matsui M, Akai Y, Konishi N, Iwano M, Nabeshima Y, and Saito Y**. Decreased renal alpha-Klotho expression in early diabetic nephropathy in humans and mice and its possible role in urinary calcium excretion. *Kidney international* 81: 539-547, 2012.
2. **Baldys A, Pande P, Mosleh T, Park SH, and Aust AE**. Apoptosis induced by crocidolite asbestos in human lung epithelial cells involves inactivation of Akt and MAPK pathways. *Apoptosis : an international journal on programmed cell death* 12: 433-447, 2007.
3. **Belov AA, and Mohammadi M**. Molecular mechanisms of fibroblast growth factor signaling in physiology and pathology. *Cold Spring Harbor perspectives in biology* 5: 2013.
4. **Bohr VA, Stevnsner T, and de Souza-Pinto NC**. Mitochondrial DNA repair of oxidative damage in mammalian cells. *Gene* 286: 127-134, 2002.
5. **Bueno M, Lai YC, Romero Y, Brands J, St Croix CM, Kamga C, Corey C, Herazo-Maya JD, Sembrat J, Lee JS, Duncan SR, Rojas M, Shiva S, Chu CT, and Mora AL**. PINK1 deficiency impairs mitochondrial homeostasis and promotes lung fibrosis. *The Journal of clinical investigation* 125: 521-538, 2015.
6. **Cheresh P, Kim SJ, Tulasiram S, and Kamp DW**. Oxidative stress and pulmonary fibrosis. *Biochimica et biophysica acta* 1832: 1028-1040, 2013.
7. **Cheresh P, Morales-Nebreda L, Kim SJ, Yeldandi A, Williams DB, Cheng Y, Mutlu GM, Budinger GR, Ridge K, Schumacker PT, Bohr VA, and Kamp DW**. Asbestos-induced pulmonary fibrosis is augmented in 8-oxoguanine DNA glycosylase knockout mice. *American journal of respiratory cell and molecular biology* 52: 25-36, 2015.
8. **Dey JH, Bianchi F, Voshol J, Bonenfant D, Oakeley EJ, and Hynes NE**. Targeting fibroblast growth factor receptors blocks PI3K/AKT signaling, induces apoptosis, and impairs mammary tumor outgrowth and metastasis. *Cancer research* 70: 4151-4162, 2010.
9. **Dolle C, Flones I, Nido GS, Miletic H, Osuagwu N, Kristoffersen S, Lilleng PK, Larsen JP, Tysnes OB, Haugarvoll K, Bindoff LA, and Tzoulis C**. Defective mitochondrial DNA homeostasis in the substantia nigra in Parkinson disease. *Nature communications* 7: 13548, 2016.
10. **Eren M, Boe AE, Murphy SB, Place AT, Nagpal V, Morales-Nebreda L, Urich D, Quaggin SE, Budinger GR, Mutlu GM, Miyata T, and Vaughan DE**. PAI-1-regulated extracellular proteolysis governs senescence and survival in Klotho mice. *Proceedings of the National Academy of Sciences of the United States of America* 111: 7090-7095, 2014.
11. **Faul C, Amaral AP, Oskouei B, Hu MC, Sloan A, Isakova T, Gutierrez OM, Aguillon-Prada R, Lincoln J, Hare JM, Mundel P, Morales A, Scialla J, Fischer M, Soliman EZ, Chen J, Go AS, Rosas SE, Nessel L, Townsend RR, Feldman HI, St John Sutton M, Ojo A, Gadegbeku C, Di Marco GS, Reuter S, Kentrup D, Tiemann K, Brand M, Hill JA, Moe OW, Kuro OM, Kusek JW, Keane MG, and Wolf M**. FGF23 induces left ventricular hypertrophy. *The Journal of clinical investigation* 121: 4393-4408, 2011.
12. **Gao W, Yuan C, Zhang J, Li L, Yu L, Wiegman CH, Barnes PJ, Adcock IM, Huang M, and Yao X**. Klotho expression is reduced in COPD airway epithelial cells: effects on inflammation and oxidant injury. *Clinical science (London, England : 1979)* 129: 1011-1023, 2015.
13. **Goetz R, Nakada Y, Hu MC, Kurosu H, Wang L, Nakatani T, Shi M, Eliseenkova AV, Razzaque MS, Moe OW, Kuro-o M, and Mohammadi M**. Isolated C-terminal tail of FGF23 alleviates hypophosphatemia by inhibiting FGF23-FGFR-Klotho complex formation. *Proceedings of the National Academy of Sciences of the United States of America* 107: 407-412, 2010.
14. **Habib SL, and Liang S**. Hyperactivation of Akt/mTOR and deficiency in tuberin increased the oxidative DNA damage in kidney cancer patients with diabetes. *Oncotarget* 5: 2542-2550, 2014.
15. **Holzenberger M, Dupont J, Ducos B, Leneuve P, Geloen A, Even PC, Cervera P, and Le Bouc Y**. IGF-1 receptor regulates lifespan and resistance to oxidative stress in mice. *Nature* 421: 182-187, 2003.
16. **Hu MC, Kuro-o M, and Moe OW**. SECRETED KLOTHO AND CHRONIC KIDNEY DISEASE. *Advances in experimental medicine and biology* 728: 126-157, 2012.
17. **Hu MC, and Moe OW**. Klotho as a potential biomarker and therapy for acute kidney injury. *Nature reviews Nephrology* 8: 423-429, 2012.
18. **Hu MC, Shi M, Zhang J, Quinones H, Kuro-o M, and Moe OW**. Klotho deficiency is an early biomarker of renal ischemia-reperfusion injury and its replacement is protective. *Kidney international* 78: 1240-1251, 2010.

19. **Hu MC, Shiizaki K, Kuro-o M, and Moe OW**. Fibroblast growth factor 23 and Klotho: physiology and pathophysiology of an endocrine network of mineral metabolism. *Annual review of physiology* 75: 503-533, 2013.
20. **Huang SX, Jaurand MC, Kamp DW, Whysner J, and Hei TK**. Role of mutagenicity in asbestos fiber-induced carcinogenicity and other diseases. *Journal of toxicology and environmental health Part B, Critical reviews* 14: 179-245, 2011.
21. **Imura A, Iwano A, Tohyama O, Tsuji Y, Nozaki K, Hashimoto N, Fujimori T, and Nabeshima Y**. Secreted Klotho protein in sera and CSF: implication for post-translational cleavage in release of Klotho protein from cell membrane. *FEBS letters* 565: 143-147, 2004.
22. **Ishii M, Yamaguchi Y, Yamamoto H, Hanaoka Y, and Ouchi Y**. Airspace enlargement with airway cell apoptosis in klotho mice: a model of aging lung. *The journals of gerontology Series A, Biological sciences and medical sciences* 63: 1289-1298, 2008.
23. **Kim SJ, Cheresh P, Jablonski RP, Morales-Nebreda L, Cheng Y, Hogan E, Yeldandi A, Chi M, Piseaux R, Ridge K, Michael Hart C, Chandel N, Scott Budinger GR, and Kamp DW**. Mitochondrial catalase overexpressed transgenic mice are protected against lung fibrosis in part via preventing alveolar epithelial cell mitochondrial DNA damage. *Free radical biology & medicine* 101: 482-490, 2016.
24. **Kim SJ, Cheresh P, Jablonski RP, Williams DB, and Kamp DW**. The Role of Mitochondrial DNA in Mediating Alveolar Epithelial Cell Apoptosis and Pulmonary Fibrosis. *International journal of molecular sciences* 16: 21486-21519, 2015.
25. **Kim SJ, Cheresh P, Williams D, Cheng Y, Ridge K, Schumacker PT, Weitzman S, Bohr VA, and Kamp DW**. Mitochondria-targeted Ogg1 and aconitase-2 prevent oxidant-induced mitochondrial DNA damage in alveolar epithelial cells. *The Journal of biological chemistry* 289: 6165-6176, 2014.
26. **Kroemer G, Galluzzi L, and Brenner C**. Mitochondrial membrane permeabilization in cell death. *Physiological reviews* 87: 99-163, 2007.
27. **Kuro-o M**. Klotho as a regulator of oxidative stress and senescence. *Biological chemistry* 389: 233-241, 2008.
28. **Kuro-o M**. Klotho in health and disease. *Current opinion in nephrology and hypertension* 21: 362-368, 2012.
29. **Kuro-o M, Matsumura Y, Aizawa H, Kawaguchi H, Suga T, Utsugi T, Ohyama Y, Kurabayashi M, Kaname T, Kume E, Iwasaki H, Iida A, Shiraki-Iida T, Nishikawa S, Nagai R, and Nabeshima YI**. Mutation of the mouse klotho gene leads to a syndrome resembling ageing. *Nature* 390: 45-51, 1997.
30. **Kurosu H, Yamamoto M, Clark JD, Pastor JV, Nandi A, Gurnani P, McGuinness OP, Chikuda H, Yamaguchi M, Kawaguchi H, Shimomura I, Takayama Y, Herz J, Kahn CR, Rosenblatt KP, and Kuro-o M**. Suppression of aging in mice by the hormone Klotho. *Science (New York, NY)* 309: 1829-1833, 2005.
31. **Larson-Casey JL, Murthy S, Ryan AJ, and Carter AB**. Modulation of the mevalonate pathway by akt regulates macrophage survival and development of pulmonary fibrosis. *The Journal of biological chemistry* 289: 36204-36219, 2014.
32. **Liu G, Cheresh P, and Kamp DW**. Molecular basis of asbestos-induced lung disease. *Annual review of pathology* 8: 161-187, 2013.
33. **Lu Y, Azad N, Wang L, Iyer AK, Castranova V, Jiang BH, and Rojanasakul Y**. Phosphatidylinositol-3-kinase/akt regulates bleomycin-induced fibroblast proliferation and collagen production. *American journal of respiratory cell and molecular biology* 42: 432-441, 2010.
34. **Lu Y, Parkyn L, Otterbein LE, Kureishi Y, Walsh K, Ray A, and Ray P**. Activated Akt protects the lung from oxidant-induced injury and delays death of mice. *The Journal of experimental medicine* 193: 545-549, 2001.
35. **Masuda H, Chikuda H, Suga T, Kawaguchi H, and Kuro-o M**. Regulation of multiple ageing-like phenotypes by inducible klotho gene expression in klotho mutant mice. *Mechanisms of ageing and development* 126: 1274-1283, 2005.
36. **Mencke R, and Hillebrands JL**. The role of the anti-ageing protein Klotho in vascular physiology and pathophysiology. *Ageing research reviews* 2016.
37. **Panduri V, Weitzman SA, Chandel NS, and Kamp DW**. Mitochondrial-derived free radicals mediate asbestos-induced alveolar epithelial cell apoptosis. *American journal of physiology Lung cellular and molecular physiology* 286: L1220-1227, 2004.
38. **Patel AS, Song JW, Chu SG, Mizumura K, Osorio JC, Shi Y, El-Chemaly S, Lee CG, Rosas IO, Elias JA, Choi AM, and Morse D**. Epithelial cell mitochondrial dysfunction and PINK1 are induced by transforming growth factor-beta1 in pulmonary fibrosis. *PloS one* 10: e0121246, 2015.
39. **Ravikumar P, Ye J, Zhang J, Pinch SN, Hu MC, Kuro-o M, Hsia CC, and Moe OW**. alpha-Klotho protects against oxidative damage in pulmonary epithelia. *American journal of physiology Lung cellular and*

molecular physiology 307: L566-575, 2014.
40. **Razzaque MS**. The FGF23-Klotho axis: endocrine regulation of phosphate homeostasis. *Nature reviews Endocrinology* 5: 611-619, 2009.
41. **Reddy NM, Potteti HR, Vegiraju S, Chen HJ, Tamatam CM, and Reddy SP**. PI3K-AKT Signaling via Nrf2 Protects against Hyperoxia-Induced Acute Lung Injury, but Promotes Inflammation Post-Injury Independent of Nrf2 in Mice. *PloS one* 10: e0129676, 2015.
42. **Satoh M, Nagasu H, Morita Y, Yamaguchi TP, Kanwar YS, and Kashihara N**. Klotho protects against mouse renal fibrosis by inhibiting Wnt signaling. *American journal of physiology Renal physiology* 303: F1641-1651, 2012.
43. **Schriner SE, Linford NJ, Martin GM, Treuting P, Ogburn CE, Emond M, Coskun PE, Ladiges W, Wolf N, Van Remmen H, Wallace DC, and Rabinovitch PS**. Extension of murine life span by overexpression of catalase targeted to mitochondria. *Science (New York, NY)* 308: 1909-1911, 2005.
44. **Selman M, and Pardo A**. Revealing the pathogenic and aging-related mechanisms of the enigmatic idiopathic pulmonary fibrosis. an integral model. *American journal of respiratory and critical care medicine* 189: 1161-1172, 2014.
45. **Soberanes S, Urich D, Baker CM, Burgess Z, Chiarella SE, Bell EL, Ghio AJ, De Vizcaya-Ruiz A, Liu J, Ridge KM, Kamp DW, Chandel NS, Schumacker PT, Mutlu GM, and Budinger GR**. Mitochondrial complex III-generated oxidants activate ASK1 and JNK to induce alveolar epithelial cell death following exposure to particulate matter air pollution. *The Journal of biological chemistry* 284: 2176-2186, 2009.
46. **Suga T, Kurabayashi M, Sando Y, Ohyama Y, Maeno T, Maeno Y, Aizawa H, Matsumura Y, Kuwaki T, Kuro OM, Nabeshima Y, and Nagai R**. Disruption of the klotho gene causes pulmonary emphysema in mice. Defect in maintenance of pulmonary integrity during postnatal life. *American journal of respiratory cell and molecular biology* 22: 26-33, 2000.
47. **Sugiura H, Yoshida T, Mitobe M, Yoshida S, Shiohira S, Nitta K, and Tsuchiya K**. Klotho reduces apoptosis in experimental ischaemic acute kidney injury via HSP-70. *Nephrology, dialysis, transplantation : official publication of the European Dialysis and Transplant Association - European Renal Association* 25: 60-68, 2010.
48. **Sugiura H, Yoshida T, Shiohira S, Kohei J, Mitobe M, Kurosu H, Kuro-o M, Nitta K, and Tsuchiya K**. Reduced Klotho expression level in kidney aggravates renal interstitial fibrosis. *American journal of physiology Renal physiology* 302: F1252-1264, 2012.
49. **Sun N, Youle RJ, and Finkel T**. The Mitochondrial Basis of Aging. *Molecular cell* 61: 654-666, 2016.
50. **Sundaresan NR, Vasudevan P, Zhong L, Kim G, Samant S, Parekh V, Pillai VB, Ravindra PV, Gupta M, Jeevanandam V, Cunningham JM, Deng CX, Lombard DB, Mostoslavsky R, and Gupta MP**. The sirtuin SIRT6 blocks IGF-Akt signaling and development of cardiac hypertrophy by targeting c-Jun. *Nature medicine* 18: 1643-1650, 2012.
51. **Thannickal VJ, Murthy M, Balch WE, Chandel NS, Meiners S, Eickelberg O, Selman M, Pardo A, White ES, Levy BD, Busse PJ, Tuder RM, Antony VB, Sznajder JI, and Budinger GR**. Blue journal conference. Aging and susceptibility to lung disease. *American journal of respiratory and critical care medicine* 191: 261-269, 2015.
52. **Trifunovic A, Wredenberg A, Falkenberg M, Spelbrink JN, Rovio AT, Bruder CE, Bohlooly YM, Gidlof S, Oldfors A, Wibom R, Tornell J, Jacobs HT, and Larsson NG**. Premature ageing in mice expressing defective mitochondrial DNA polymerase. *Nature* 429: 417-423, 2004.
53. **Upadhyay D, Bundesmann M, Panduri V, Correa-Meyer E, and Kamp DW**. Fibroblast growth factor-10 attenuates H2O2-induced alveolar epithelial cell DNA damage: role of MAPK activation and DNA repair. *American journal of respiratory cell and molecular biology* 31: 107-113, 2004.
54. **Wang H, Liao S, Geng R, Zheng Y, Liao R, Yan F, Thrimawithana T, Little PJ, Feng ZP, Lazarovici P, and Zheng W**. IGF-1 signaling via the PI3K/Akt pathway confers neuroprotection in human retinal pigment epithelial cells exposed to sodium nitroprusside insult. *Journal of molecular neuroscience : MN* 55: 931-940, 2015.
55. **Wolf I, Levanon-Cohen S, Bose S, Ligumsky H, Sredni B, Kanety H, Kuro-o M, Karlan B, Kaufman B, Koeffler HP, and Rubinek T**. Klotho: a tumor suppressor and a modulator of the IGF-1 and FGF pathways in human breast cancer. *Oncogene* 27: 7094-7105, 2008.
56. **Wu KI, Pollack N, Panos RJ, Sporn PH, and Kamp DW**. Keratinocyte growth factor promotes alveolar epithelial cell DNA repair after H2O2 exposure. *The American journal of physiology* 275: L780-787, 1998.
57. **Xia H, Diebold D, Nho R, Perlman D, Kleidon J, Kahm J, Avdulov S, Peterson M, Nerva J, Bitterman P, and Henke C**. Pathological integrin signaling enhances proliferation of primary lung fibroblasts from patients with idiopathic pulmonary fibrosis. *The Journal of experimental medicine* 205: 1659-1672, 2008.
58. **Yamamoto M, Clark JD, Pastor JV, Gurnani P, Nandi A, Kurosu H, Miyoshi M, Ogawa Y, Castrillon**

DH, Rosenblatt KP, and Kuro-o M. Regulation of oxidative stress by the anti-aging hormone klotho. *The Journal of biological chemistry* 280: 38029-38034, 2005.

59. **Yang K, Wang C, Nie L, Zhao X, Gu J, Guan X, Wang S, Xiao T, Xu X, He T, Xia X, Wang J, and Zhao J**. Klotho Protects Against Indoxyl Sulphate-Induced Myocardial Hypertrophy. *Journal of the American Society of Nephrology : JASN* 26: 2434-2446, 2015.

60. **Zeldich E, Chen CD, Colvin TA, Bove-Fenderson EA, Liang J, Tucker Zhou TB, Harris DA, and Abraham CR**. The neuroprotective effect of Klotho is mediated via regulation of members of the redox system. *The Journal of biological chemistry* 289: 24700-24715, 2014.

Figure 1

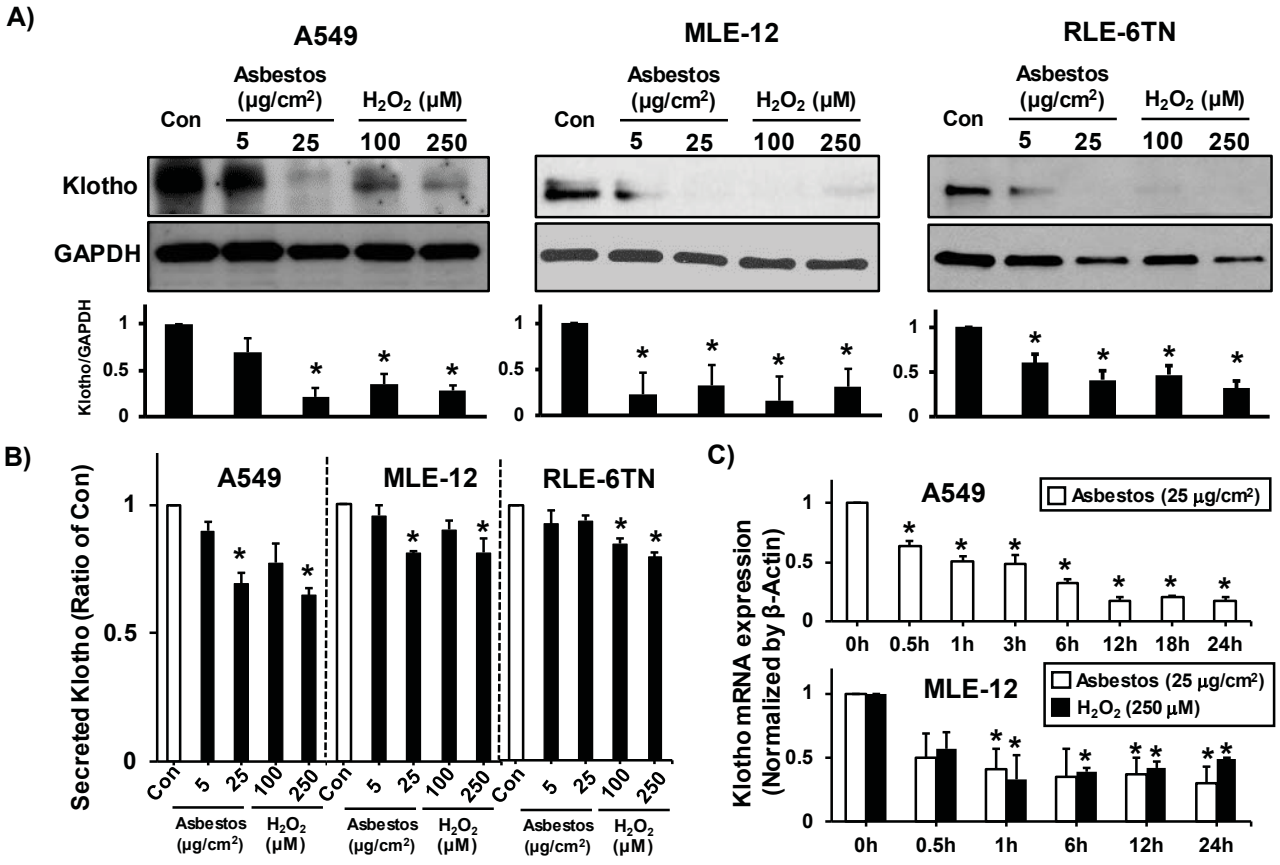
A)
A549
MLE-12
RLE-6TN
Asbestos (μg/cm²)
H₂O₂ (μM)
Con
5
25
100
250
Klotho
GAPDH
Klotho/GAPDH
B)
Secreted Klotho (Ratio of Con)
C)
Klotho mRNA expression (Normalized by β-Actin)
Asbestos (25 μg/cm²)
H₂O₂ (250 μM)
0h
0.5h
1h
3h
6h
12h
18h
24h

Figure 2

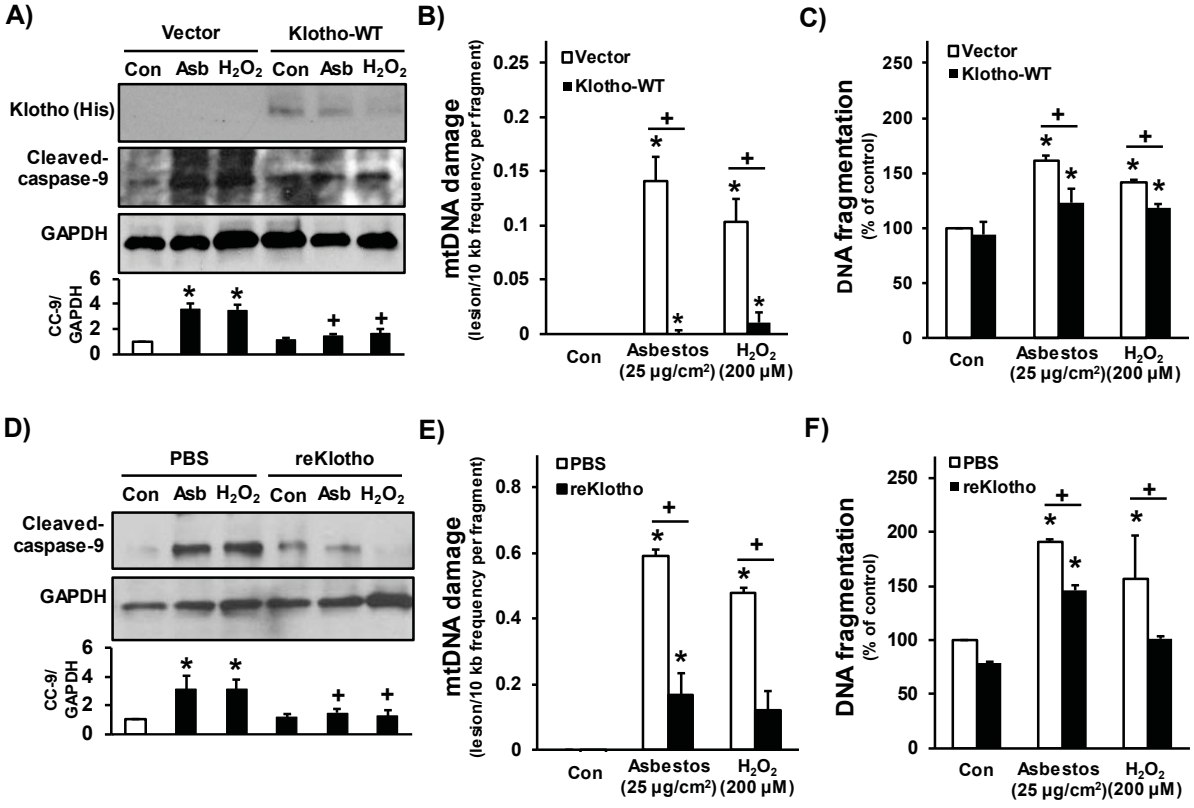
A)
Vector
Klotho-WT
Con Asb H2O2 Con Asb H2O2
Klotho (His)
Cleaved-caspase-9
GAPDH
CC-9/GAPDH
B)
Vector
Klotho-WT
mtDNA damage
(lesion/10 kb frequency per fragment)
Con
Asbestos (25 μg/cm2)
H2O2 (200 μM)
C)
Vector
Klotho-WT
DNA fragmentation
(% of control)
Con
Asbestos (25 μg/cm2)
H2O2 (200 μM)
D)
PBS
reKlotho
Con Asb H2O2 Con Asb H2O2
Cleaved-caspase-9
GAPDH
CC-9/GAPDH
E)
PBS
reKlotho
mtDNA damage
(lesion/10 kb frequency per fragment)
Con
Asbestos (25 μg/cm2)
H2O2 (200 μM)
F)
PBS
reKlotho
DNA fragmentation
(% of control)
Con
Asbestos (25 μg/cm2)
H2O2 (200 μM)

Figure 3

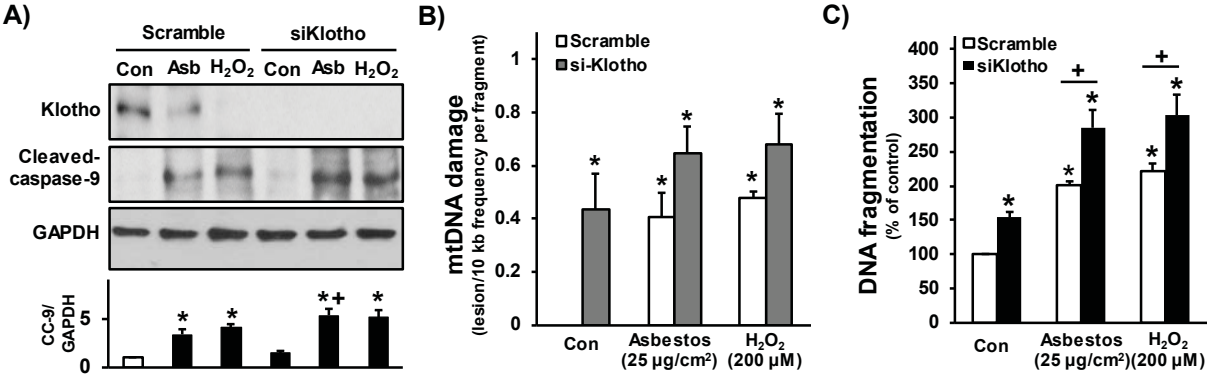
A)
Scramble
siKlotho
Con
Asb
H2O2
Con
Asb
H2O2
Klotho
Cleaved-caspase-9
GAPDH
CC-9/GAPDH
5
0
B)
Scramble
si-Klotho
mtDNA damage
(lesion/10 kb frequency per fragment)
1
0.8
0.6
0.4
0.2
0
Con
Asbestos (25 μg/cm2)
H2O2 (200 μM)
C)
Scramble
siKlotho
DNA fragmentation
(% of control)
400
350
300
250
200
150
100
50
0
Con
Asbestos (25 μg/cm2)
H2O2 (200 μM)

Figure 4

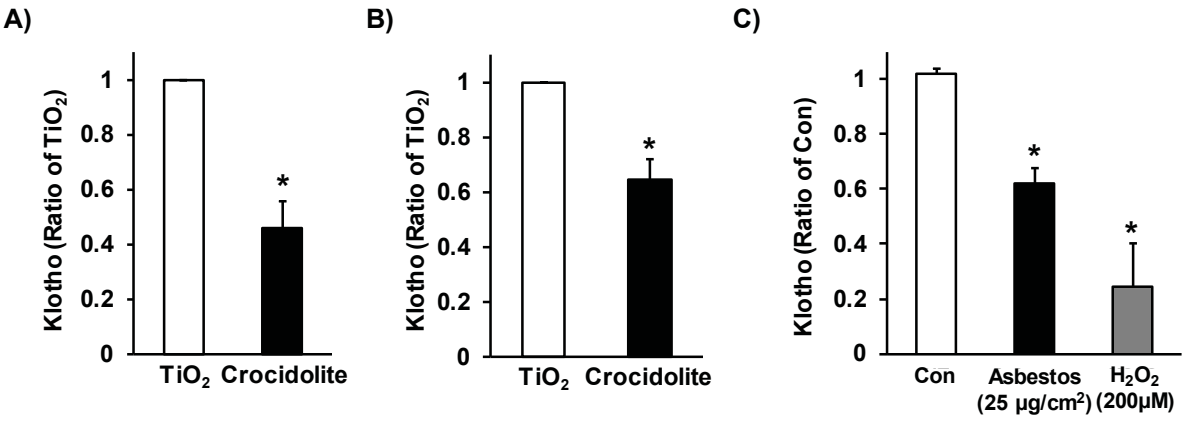
A)
B)
C)
Klotho (Ratio of TiO2)
Klotho (Ratio of Con)
1
0.8
0.6
0.4
0.2
0
*
TiO2
Crocidolite
Con
Asbestos
(25 μg/cm2)
H2O2
(200μM)

Figure 5

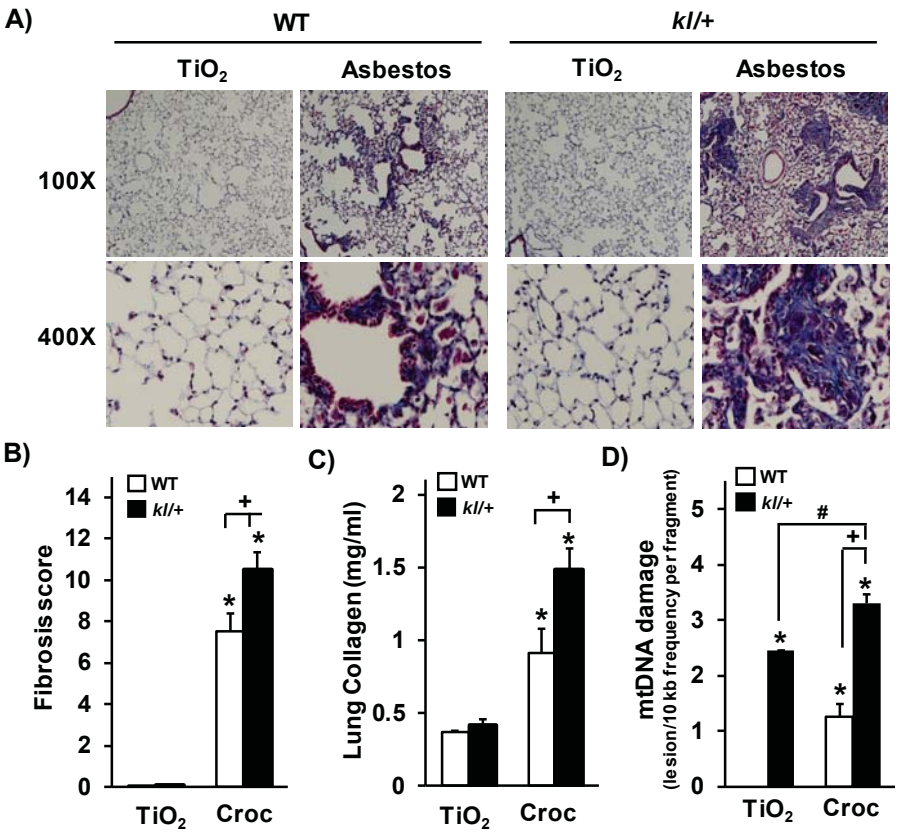
A)
WT
kl/+
TiO2
Asbestos
TiO2
Asbestos
100X
400X
B)
WT
kl/+
Fibrosis score
TiO2
Croc
C)
WT
kl/+
Lung Collagen (mg/ml)
TiO2
Croc
D)
WT
kl/+
mtDNA damage
(lesion/10 kb frequency per fragment)
TiO2
Croc

Figure 6

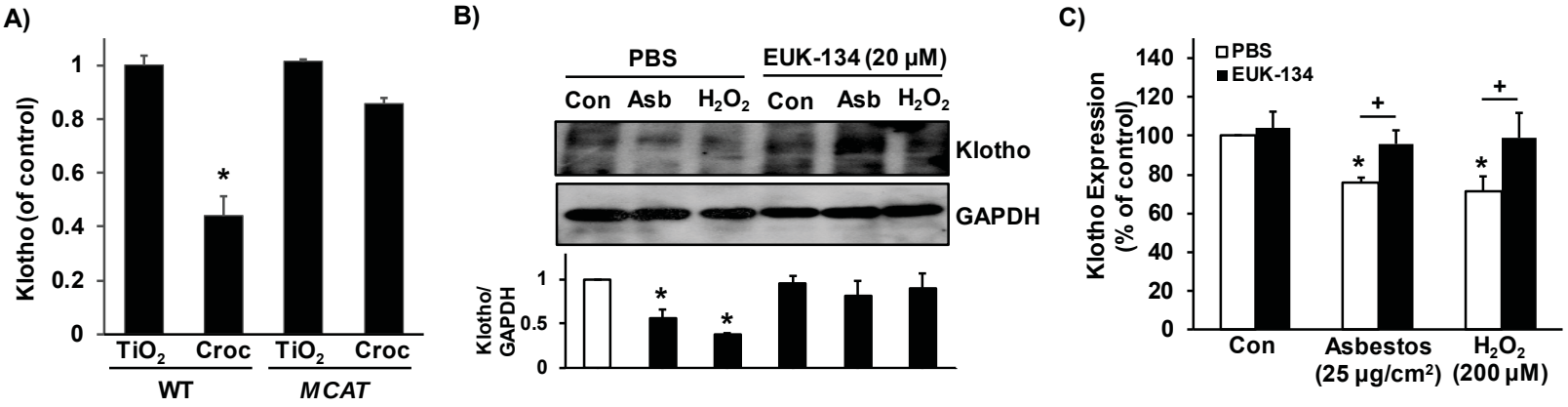
A)
Klotho (of control)
1
0.8
0.6
0.4
0.2
0
*
TiO2
Croc
TiO2
Croc
WT
MCAT
B)
PBS
EUK-134 (20 μM)
Con
Asb
H2O2
Con
Asb
H2O2
Klotho
GAPDH
Klotho/ GAPDH
1
0.5
0
*
*
C)
PBS
EUK-134
Klotho Expression (% of control)
140
120
100
80
60
40
20
0
*
+
*
+
Con
Asbestos (25 μg/cm2)
H2O2 (200 μM)

Figure 7

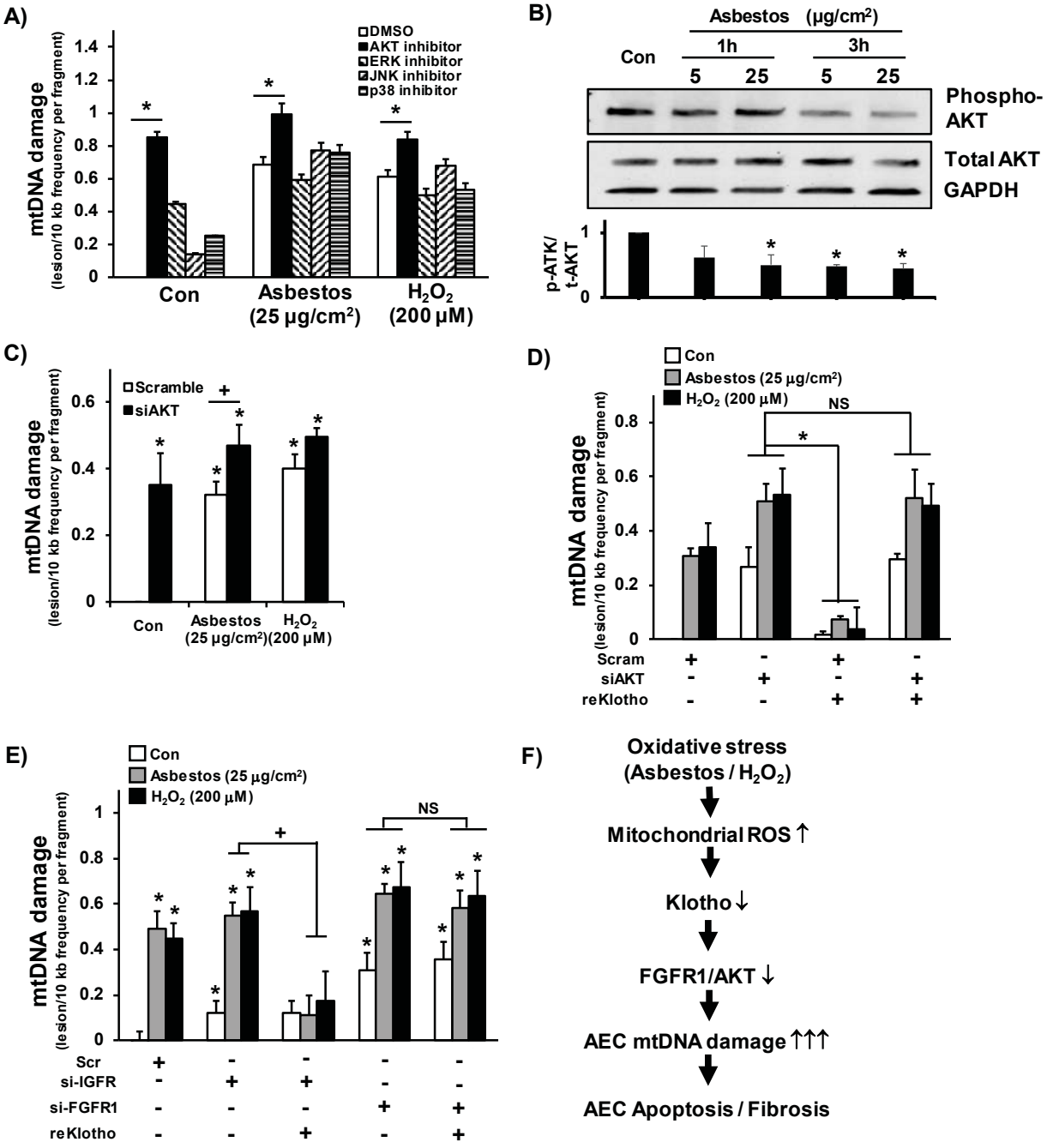
A)
mtDNA damage
(lesion/10 kb frequency per fragment)
DMSO
AKT inhibitor
ERK inhibitor
JNK inhibitor
p38 inhibitor
Con
Asbestos (25 μg/cm²)
H2O2 (200 μM)
B)
Asbestos (μg/cm²)
Con
1h
3h
5
25
5
25
Phospho-AKT
Total AKT
GAPDH
p-ATK/ t-AKT
C)
Scramble
siAKT
Con
Asbestos (25 μg/cm²)
H2O2 (200 μM)
D)
Con
Asbestos (25 μg/cm²)
H2O2 (200 μM)
NS
Scram
siAKT
reKlotho
E)
Con
Asbestos (25 μg/cm²)
H2O2 (200 μM)
NS
Scr
si-IGFR
si-FGFR1
reKlotho
F)
Oxidative stress
(Asbestos / H2O2)
Mitochondrial ROS ↑
Klotho ↓
FGFR1/AKT ↓
AEC mtDNA damage ↑↑↑
AEC Apoptosis / Fibrosis